Aspartate Aminotransferase Complexed with *erythro*-β-Hydroxyaspartate: Crystallographic and Spectroscopic Identification of the Carbinolamine Intermediate‡

Andreas Graf von Stosch*

Harleβstr. 14, D-40239 Düsseldorf, Germany

Received April 25, 1996; Revised Manuscript Received September 23, 1996⊗

ABSTRACT: The crystal structure of mitochondrial aspartate aminotransferase (mAAT) of chicken complexed with *erythro*-β-hydroxyaspartate has been determined at 2.4 Å resolution. Pregrown crystals of mAAT complexed with the inhibitor maleate (closed enzyme conformation, orthorhombic space group $C222_1$) were soaked in solutions of *erythro*-β-hydroxyaspartate. The ligand exchange was monitored by microspectrophotometry. The active site turned out to be predominantly occupied by the carbinolamine intermediate. The carbinolamine is a true intermediate of the catalytic cycle forming the last covalently bound enzyme:substrate complex before release of the keto acid product. Occupancies of approximately 80% for the carbinolamine and of approximately 20% for the quinonoid intermediate were obtained. Two hydrogen bonds were identified that are potentially relevant for the accumulation of the carbinolamine intermediate: one to the hydroxyl group of Tyr 70* and the other to the ϵ-NH_2 group of Lys 258.

Aspartate:2-oxoglutarate aminotransferase (E.C. 2.6.1.1; abbreviated AAT) is one of the best-studied vitamin B_6-dependent enzymes (Braunstein, 1973; Christen & Metzler, 1985). It is a symmetrical, α_2-dimeric enzyme with a subunit mass of approximately 45 000 Da. AAT dimers possess two functional active sites, both located at the monomer−monomer interface and composed of residues from each subunit. Pyridoxal-5′-phosphate (PLP), the physiological active form of vitamin B_6 (pyridoxine), is a necessary cofactor for AAT-catalyzed transamination. The PLP molecule is linked to the ϵ-NH_2 of lysine 258 through a Schiff base in native AAT (internal aldimine; Hughes et al., 1962).

AAT catalyzes the enzymatic transfer by a "ping-pong bi-bi" mechanism (Cleland, 1963). In the first half-reaction, L-aspartate binds to the enzyme, the PLP coenzyme is aminated to pyridoxamine-5′-phosphate (PMP), and oxalocetate is released as product. During the reverse reaction, the transamination cycle is completed by transferring the amino group of PMP to 2-oxoglutarate, which leads to L-glutamate. The catalytic mechanism of AAT involves minimally seven intermediates, which were originally detected by Fasella and Haslam (1967) using UV/visible absorption spectroscopy in kinetic studies. The first half-reaction, starting with the PLP enzyme, can be described as follows (Figure 1). Lysine 258 forms a Schiff base (internal aldimine **1**) with the 4′-carbon atom of the coenzyme in the resting, unliganded enzyme. The aldimine nitrogen has an apparent pK_a value of approximately 6.3 and is normally deprotonated under physiological conditions. Binding of amino acid substrates causes a pK_a shift of the aldimine (to a more alkaline value) leading to a proton transfer from the charged amino group on the substrate to the aldimine nitrogen, giving the Michaelis complex **2**. As a consequence of the proton shift, a nucleophilic attack of the substrate on the 4′-carbon rapidly follows. A tetrahedral intermediate (geminal diamine **3**) results and reacts further to the external aldimine **4**. At this stage the uncharged ϵ-amino group is free of covalent interactions with the coenzyme. The next step demonstrates the crucial role of lysine 258 during transamination, the Cα-proton on the substrate moiety is removed by the ϵ-NH_2 group, producing the quinonoid intermediate **5** which is stabilized by an extended, conjugated double-bond system (Snell, 1962; Ivanov & Karpeisky, 1969). The 1,3-azaallylic rearrangement (or 1,3-prototropic shift) is completed when lysine 258 protonates the quinonoid at the 4′-carbon, regenerating the aromatic ring character of the pyridine ring. The ketimine **6** is hydrolyzed by a water molecule via a carbinolamine intermediate (**7**) to enzyme-bound PMP and the oxo acid product, the latter being rapidly released (**8**) (Ivanov & Karpeisky, 1969; Christen & Metzler, 1985; Jansonius & Vincent, 1987).

A major tool in enzymatic and crystallographic studies is the application of quasi-substrates and inhibitors. To date, a large number of substrate analogues for mitochondrial and cytosolic AAT has been introduced. Some of these mimic intermediates of enzymatic transamination, while others explore binding and reactivity in the active site (Harutyunyan et al., 1985; Arnone et al., 1985; Malashkevich et al., 1991; Ford et al., 1980; McPhalen et al., 1992; Malashkevich et al., 1993).

erythro-β-Hydroxyaspartate is a poor substrate that displays an accumulation of the quinonoid intermediate during catalysis. This inhibitor was discovered in 1960 by chance, when Jenkins (1961) reported an intense light absorption band at 492 nm with pure cytosolic aspartate aminotransferase and an impurity present in glycine. This impurity turned out to be *erythro*-β-hydroxyaspartate. This compound differs from the native substrate L-aspartate by an additional hydroxyl group at the β-carbon atom (Figure 2). Crystallographic studies with this quasi-substrate were previously performed at low resolution (Picot, 1987). Hammes and Haslam (1969) performed rapid reaction kinetic experiments, while others (Picot, 1987; Metzler, 1988a,b) have examined

* Corresponding author. Fax: ++49/211/9146060. Tel: ++49/211/615563.

‡ The coordinates of the refined structure have been deposited under Filename 1IVR with the Brookhaven Protein DataBank, Brookhaven National Laboratory, Upton, NY.

⊗ Abstract published in *Advance ACS Abstracts,* November 1, 1996.

S0006-2960(96)00994-4 CCC: $12.00

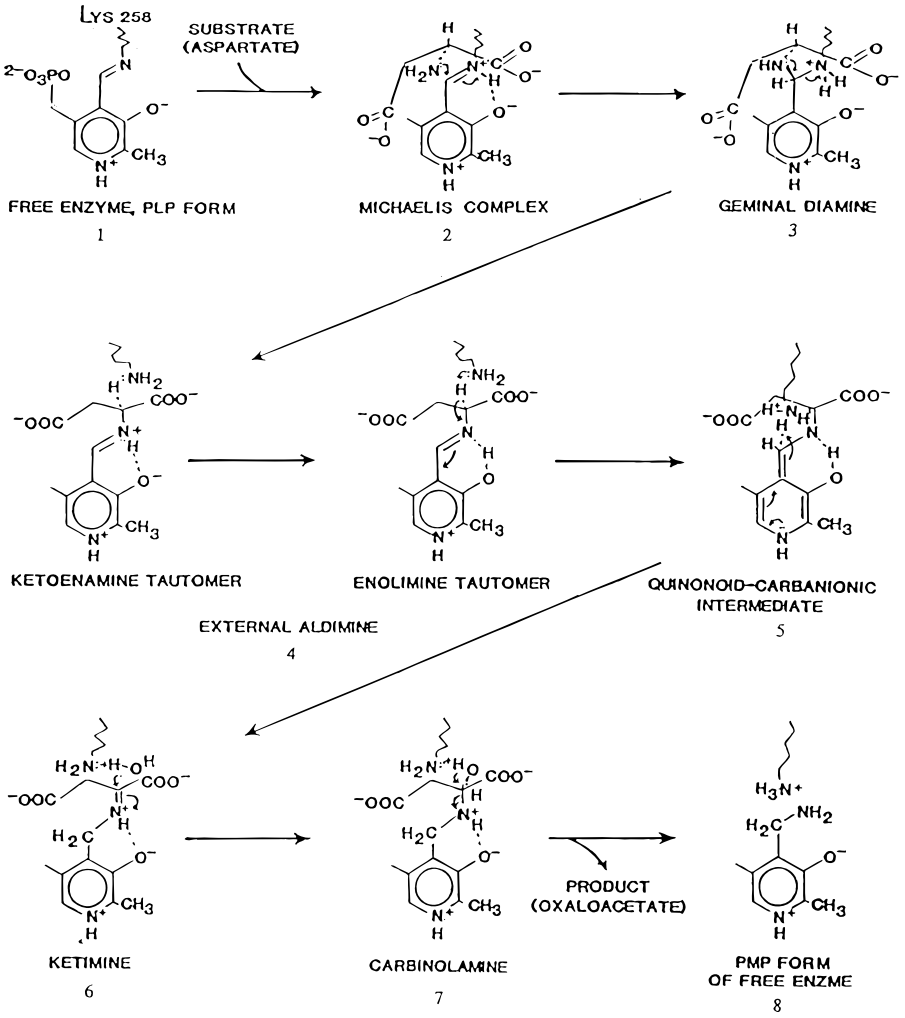

FIGURE 1: Reaction scheme for a half-reaction of aspartate aminotransferase with aspartate to produce oxaloacetate. The role of Lys 258 and its state of protonation is emphasized (Metzler, 1979).

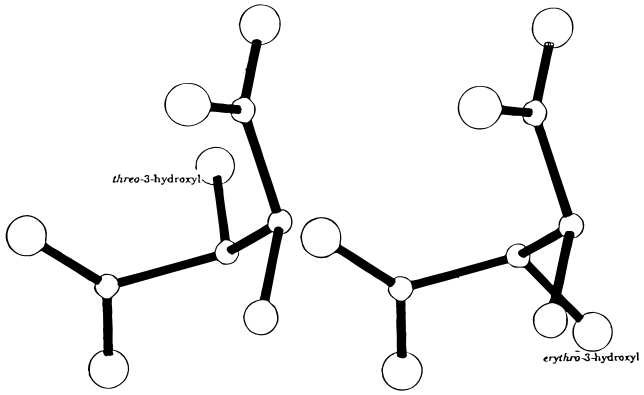

FIGURE 2: Diastereoisomers *erythro*- and *threo*-3-L-hydroxyaspartate. They are distinguished by different chiralities around the Cβ atom.

AAT complexed with *erythro*-β-hydroxyaspartate with UV/visible absorption spectroscopy. Taylor et al. (1990) applied molecular dynamics calculations to model *erythro*-β-hydroxyaspartate into the active site.

The subject of this paper is the high-resolution structure determination of mitochondrial AAT (mAAT) from chicken complexed with *erythro*-β-hydroxyaspartate and the interpretation of the crystallographic results in the context of previous kinetic and spectroscopic studies. Orthorhombic crystals ($C222_1$) complexed with *erythro*-β-hydroxyaspartate were used in the present study. The crystals have one subunit per asymmetric unit, which means that the molecular dyad is coincident with a crystallographic 2-fold axis. The unit cell axes are $a = 69.7$, $b = 91.4$, and $c = 128.5$ Å.

MATERIALS AND METHODS

Preparation of erythro-β-Hydroxyaspartate. *erythro*-β-Hydroxyaspartate was enzymatically prepared according to a method proposed by Jenkins (1979). The synthesis of hydroxyaspartate, including both diastereomers (*erythro*- and *threo*-forms, Figure 2), was catalyzed by pig heart aspartate aminotransferase and tris(hydroxymethyl)aminomethane buffer. Cysteinesulfinate was used as the amino group donor, and dihydroxyfumarate served as the amino group acceptor for aspartate aminotransferase. Dihydroxyfumarate is the enol form of oxaloglycolate, the keto acid corresponding to β-hydroxyaspartate. All attempts to characterize the keto form failed because of its fast tautomerization to the stable enol form. Tris served as a base to catalyze the ketonization. Since the enzyme reacts only with the L-amino acids (observed for all substrates and inhibitors of AAT), two instead of four diastereomers are found as the products of transamination. These were separated by a column of DOWEX 1-X8 (formate, 50−100 mesh). The advantage of this method over chemical synthesis is to prepare *erythro*-β-L-hydroxyaspartate without any contamination by the D-isomer. However, relatively large amounts of transaminase

are required because of the low turnover number (1 s^{-1}) for this pseudosubstrate (Haruff & Jenkins, 1978). The preparation of *erythro*-β-hydroxyaspartate was carried out by Dr. M. Toney at the University of California, Berkeley.

Preparation of Crystals. The conditions for crystallization of chicken mAAT are well established, and crystals have been successfully obtained in many laboratories. The general procedure for crystallization of AAT in the orthorhombic crystal form with ligands (Picot, 1987; Picot et al., 1991) is similar to that employed in previous work on triclinic and monoclinic crystals (Gehring et al., 1977; Eichele, 1980) using the hanging drop vapor diffusion technique (McPherson, 1976, 1982).

The crystallization drop was formed by mixing 5 μL of chicken mAAT (10 mg/mL) and maleate (100 mM) as cocrystallizing inhibitor in sodium phosphate buffer (20 mM) at pH 7.5 with 5 μL of 17−19% (w/v) poly(ethylene glycol) (PEG), molecular mass 4000 Da, in a similar buffer as above but additionally containing 0.75 M sodium chloride. The drops were deposited on siliconized coverslips, which were subsequently placed over multiwell tissue culture plates and sealed with vacuum grease. Each well contained 1 mL of 17−19% (w/v) PEG precipitant solution with 20 mM sodium phosphate (pH 7.5) and 0.75 M sodium chloride. After a few days at 4 °C, yellow crystals of various shapes appeared. Platelike as well as needle-shaped and bladed crystals were observed.

Soaking Experiments. The replacement of cocrystallized inhibitors in solutions of other substrate-like inhibitors is an alternative way to complex enzymes with substrate analogues (Eichele et al., 1979; Kirsch et al., 1984; Picot, 1987; Picot et al., 1991). The pregrown crystals of chicken mAAT complexed with maleate were soaked in solutions of *erythro*-β-hydroxyaspartate. Previous cocrystallization experiments with *erythro*-β-hydroxyaspartate failed, since this pseudosubstrate undergoes transamination in solution and even in triclinic crystals (Eichele et al., 1978; Picot, 1987).

In order to avoid disruption of the crystal, it proved necessary to choose a stepwise procedure, gradually lowering the maleate and increasing the *erythro*-β-hydroxyaspartate concentration. The crystals were transferred by pipet from one solution to another of higher inhibitor concentration. For the soaking experiment, it is important to note that (i) the PEG concentration was never lower than 20% (w/v) (otherwise, the crystals lose their yellow color and start to dissolve), (ii) a soaking time of 5−10 min in each solution should not be exceeded (the longer the crystals are exposed to the soaking solution, the more apparent becomes crystal damage), and (iii) dihydroxyfumarate, the transamination product of *erythro*-β-hydroxyaspartate, was added to the soaking solution. Dihydroxyfumarate is in equilibrium with oxaloglycolate, the presence of which ensures that no unliganded PMP enzyme exists in the crystals (M. Toney, personal communication).

Microspectrophotometry of Crystals of Chicken mAAT. A Zeiss microspectrophotometer linked to a HP9845 B microprocessor was used for recording polarized as well as unpolarized absorption spectra. The Zeiss λ-SCAN program package allows control of the measurement setup and the recording procedure. A xenon lamp XB075 served as light source in conjunction with a grating monochromator. In order to orient the crystals correctly with respect to the polarized light beam, the crystal samples were placed on a rotating table that lies between the condenser and an objective lens. The transmitted light passes through a measuring diaphragm and is finally intercepted by a photomultiplier. The crystals were transferred with a drop of suitable buffer onto a microscope slide.

In the orthorhombic crystals, the principal axes of the absorption ellipsoid are coincident with the crystal axes (Hartshorne & Stuart, 1969). Spectra were measured with the light polarized parallel to the *a* and *c* crystallographic axes (A_a and A_c, respectively), the incident light beam being normal to the (010) face. Spectra were normally recorded between 270 and 550 nm in steps of 2 nm. The surrounding buffer solution served in all cases as standard reference, and reference spectra were recorded in the immediate vicinity of the crystal. Crystals of an average size of 0.07 × 0.05 × 0.2 mm were suitable for recording absorption spectra.

The estimation of occupancies of various coenzyme: substrate species within the crystal were made according to the approximation given by the "oriented gas theory" (Craig & Walmsley, 1968).

X-ray Data Collection

Experimental Setup. A platelike crystal of 0.15 × 0.4 × 1.2 mm was used for the X-ray data collection. The crystal was mounted in a thin-walled capillary of 1 mm diameter. A small amount of buffer was introduced into the capillary in order to avoid drying out of the crystal. The capillary was then sealed with beewax at both ends.

X-ray data collection was performed using an area detector diffractometer (FAST, Enraf-Nonius, Delft) controlled by a micro-VAX 3500. The rotating anode generator was operated at 40 kV and 70 mA. The Cu Kα radiation (1.5418 Å) was monochromated using graphite. The beam was collimated to 0.4 mm in diameter. For data collection, a distance of 85 mm and a swing-out angle of −21° were chosen to record reflections from resolutions of 10−2.3 Å.

Data Acquisition. The MADNES (Munich Area Detector NE Software) software package (Messerschmidt & Pflugrath, 1987) was employed for data collection and data evaluation. The glass capillary was mounted onto the goniometer of the FAST with the crystal *a*-axis (long needle axis) approximately parallel to the rotation axis (around Ω). The data were collected using the BRUTE FORCE (BF) option with the MADNES on-line version MONL. The images were dumped on disk, no spots were predicted, and no evaluation or refinement was done.

The collection method used in MADNES in conjunction with the area detector highly resembles that used for oscillation photographs. The crystal was rotated around the Ω axis in small steps (increment $\Delta\varphi = 0.15°$). One Ω scan of 110° was performed in the course of the "main" data collection. For collecting "cusp" data, an orientation perpendicular to the equivalent "main" setting is needed. A second scan, now with the *c*-axis approximately parallel to the rotation axis, measured the reflections of the blind region ("cusp region") comprising 22°. Each image was exposed for 150 s.

Data Evaluation. In order to find the orientation of the mounted crystal, the autoindexing option (algorithm by P. Tucker) was applied (FIND level, AUTOIDX level). Two 3° sections of reciprocal space from 0° to 3° and from 90° to 93° in steps of 0.15° were collected. To find reflections,

Table 1: Compositions of the Solutions Used for the Stepwise Crystal-Soaking Experiments for Exchange of Maleate against *erythro*-β-Hydroxyaspartate

	1	2	3	4	5	6	7
NaP buffer	pH 7.5 20 mM	pH 7.5 20 mM	pH 7.5 20 mM	20 mM	pH 7.5 20 mM	pH 7.5 20 mM	pH 7.5 20 mM
PEG (w/v)	17−19%	17−19%	30%	30%	32%	30%	28%
NaCl	0.75 M	0.75 M	0.6 M	0.6 M	0.6 M	0.6 M	0.6 M
maleate	100 mM	100 mM	48 mM	22 mM	7 mM	3 mM	
erythro-3-hydroxyaspartate		1.9 mM	8 mM	20 mM	30 mM	32 mM	31 mM
dihydroxyfumarate			1 mM	4 mM	4 mM	4 mM	8 mM

MADNES searches through consecutive images for reflections more than 5σ above the average background level (FIND level). Three-dimensional coordinates (x, y, position of the spots on the detector surface; φ, rotation angle) are obtained for the spots. The AUTOIDX level assigns Miller indices (hkl) to the reflections found according to the orientation matrix. The orientation matrix is determined by a trial-and-error method comparing calculated difference vectors (obtained by a trial orientation matrix) with difference vectors of previously found spots. Subsequent refinement of cell dimensions, crystal to detector distance, orientation matrix, and mosaic spread terminate the exact determination of the orientation matrix (REFINE level).

Calculation of Electron Densities, Modeling, and Refinement. The structures of chicken mAAT complexed with maleate and α-methylaspartate have been solved and refined (Jansonius & Vincent, 1987). They were expected to differ from the *erythro*-β-hydroxyaspartate complex only slightly. Structural differences by the inhibitor replacement were anticipated in the active site. The α-methylaspartate structure (resolution 2.3 Å, $R = 15.9\%$) was chosen as the starting model for supplying phase information. In order to avoid any bias by the coenzyme:α-methylaspartate complex, all of its atoms were removed from the model, before calculation of structure factors (with the program GENSFC).

The PROLSQ package [protein refinement of least-squares, written by Hendrickson and Konnert (1980)] was employed for refinement of coordinates and subsequent refinement of temperature factors (B-factors). In order to save computing time, a modified version of PROLSQ was used (developed by T. Schirmer) considering only a defined sphere of the protein ("local refinement"). The coordinates of the enzyme were divided into two zones: (i) An "active" sphere (radius 12 Å) was defined around the 4′-carbon of the coenzyme; within this sphere atoms of the outer shell of 3 Å were "frozen", whereas the atoms of the inner sphere of 9 Å were actually considered for refinement; and (ii) all atoms outside of the 12 Å sphere were kept constant and written in a separate coordinate file.

TNT (written by Ten Eyck & Tronrud), like PROLSQ, is also a restrained least-squares refinement package. The TNT package was only used to refine B-factors, positional parameters, and occupancies of the coenzyme and its covalently bound ligand. It was applied in order to refine two alternative conformations within the electron density for the coenzyme and the substrate.

RESULTS

Soaking Experiments. The cocrystallized inhibitor maleate was largely exchanged for *erythro*-β-hydroxyaspartate within seconds, but slight absorption changes still appeared 45 min after starting the soaking experiment. The inhibitor exchange was monitored by the change of crystal color. The enzyme:maleate complex is faintly yellow in color, whereas crystals complexed with *erythro*-β-hydroxyaspartate show an intense golden-yellow color. The spectra of AAT with maleate lost their 440 nm absorption band during soaking and produced an absorption spectrum with maxima at 330, 380, and 460/490 nm. The latter spectrum did not change for several days in the present experiments. These results are corroborated by those of D. Picot (1987), who observed complex stability over months. This condition is necessary for successful X-ray data collection, since crystalline AAT generally is catalytically competent for substrates.

A gradual soaking procedure proved that the crystals could remain intact for crystallographic analysis. Raising the PEG concentration supported the crystal stability. Several crystals were tested for their scattering ability. No crystal diffracted X-rays to better than 2.3 Å resolution (Table 1).

Microspectrophotometry. Coenzyme bound to AAT exhibits absorption bands ($\pi \rightarrow \pi^*$ transitions) in the near-UV. Linearly polarized and unpolarized light spectra of crystals of the mAAT:maleate complex and of the same crystals after soaking in solutions of *erythro*-β-hydroxyaspartate were recorded (Figure 3). The 280 nm band is due to the absorption of aromatic amino acid side chains. Upon binding of maleate the 360 nm peak, which represents the unprotonated internal aldimine, is shifted to the strong 442 nm band. The enzyme now adopts the closed conformation. The interpretation of this inhibitor complex as the protonated internal aldimine, mimicking the Michaelis complex, is consistent with X-ray crystallography and cryoenzymological studies (Gehring, 1986). A pK_a shift of the imine nitrogen from approximately 6.3 (Jenkins, 1959) to a more alkaline value leads to its protonation. This shift is caused by the binding of a dicarboxylic acid that compensates the positive charges of Arg 386 and Arg 292*. For the present study, the unpolarized light spectrum and especially the three linearly polarized light absorption spectra of the orthorhombic crystal soaked in *erythro*-β-hydroxyaspartate along the orthogonal crystal axes (A_a, A_b, A_c) are of interest. They were used to estimate relative proportions of two different coenzyme:ligand structures with this substrate analogue. The measured spectra agree with those of former studies (Picot, 1987; Mitra et al., 1989).

On soaking crystals in *erythro*-β-hydroxyaspartate, the 335 and 440 nm absorption bands of the maleate complex were rapidly (within a few seconds) replaced with three new ones (330, 380, and 490 nm with a shoulder at 460 nm). The 490 nm peak with its prominent shoulder on the high-energy side has been assigned to the quinonoid structure (Jenkins, 1961, 1964; Schirch & Slotter, 1966; Picot, 1987). Metzler and Metzler (1987) analyzed this absorption band with cAAT in solution and performed a lognormal curve fitting. They found that the sum of three nearly Gaussian curves ap-

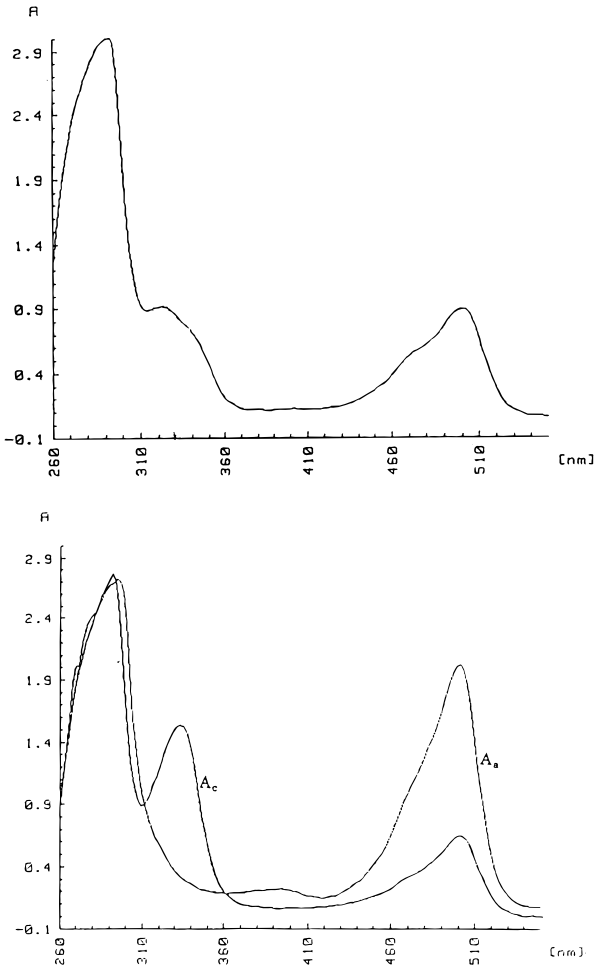

FIGURE 3: (Top) Unpolarized absorption spectrum of a maleate:mAAT crystal soaked in solutions of *erythro*-β-hydroxyaspartate (last solution: 40 mM *erythro*-β-hydroxyaspartate). The 280 nm band is due to absorption properties of amino acid side chains. (Bottom) Polarized absorption spectra of a maleate:mAAT crystal soaked in solutions of *erythro*-β-hydroxyaspartate. Spectra measured along the the crystallographic *a*- and *c*-axes are shown. The bands with a maximum around 280 nm are due to absorption properties of amino acid side chains. A band at 380 nm was detected in the absorption spectrum of AAT complexed with *erythro*-β-hydroxyaspartate measured along the *a*-axis. From its dichroic ratio, the TDM is near to those derived from the 460 and 490 nm bands of the quinonoid intermediates (Picot, 1987). Although there were some indications that small amounts of unliganded PLP (absorbing partly at 390 nm and partly at lower wavelengths) cause this absorption (Metzler et al., 1988b), the origin of the 380 nm peak could not unambiguously be attributed until now.

proximates well the observed 460/490 nm peak. These likely represent different vibrational states of the quinonoid.

A second band was recorded at a maximum around 330 nm. The 330 nm band cannot be assigned uniquely to a single species by spectroscopic methods due to the similar absorption of the PMP, ketimine, and carbinolamine forms. Their transition dipole moments (TDM) coincide near the C2−C5 axis of the coenzyme pyridine ring. This axis corresponds in a first approximation to the rotation axis of the coenzyme during catalysis (Karpeisky & Ivanov, 1966). Therefore, linear dichroism experiments cannot distinguish between these structures absorbing at 330 nm (Picot, 1987). Similarly, the source of the 380 nm absorption has not been assigned.

The relative proportions of the component(s) absorbing around 330 and 490 nm (the quinonoid) were estimated according to the oriented gas theory (Craig & Walmsley, 1968). The molar absorptivity of the latter was assumed to be 41 000 M^{-1} cm^{-1} in solution (Ulevitch & Kallen, 1977), whereas a value of 8000 M^{-1} cm^{-1} was claimed for the 330 nm compound(s). The spectra shown in Figure 3 and those measured by Picot (1987) were used for the calculations. A ratio of approximately 6:1 was obtained, suggesting that around 85% of the crystal complexed with *erythro*-β-hydroxyaspartate is occupied by the structures absorbing at 330 nm and only 15% by the 490 nm absorbing quinonoid species. Another approach to estimate the relative proportions using the unpolarized light spectrum led to very similar results (83%/17%).

X-ray Data Evaluation. Reflections of a resolution higher than 2.4 Å were excluded from further evaluation (R_{sym} = 39%). Neglecting these reflections, the accumulated R_{sym} was 8.6%. The rejection of the 2.4−2.3 Å resolution shell is based on the assumption that the statistical error of reflections with R_{sym} higher than 35% is too large. The reflections observed represented 86.4% of the unique data set.

Refinement. The refined structure of mAAT complexed with α-methylaspartate served as a starting model for the refinement procedure. The atoms of the coenzyme, the ligand, and the side chain of Lys 258 were omitted for the calculation of the first difference electron density map. As expected, the highest positive density in this initial omit map, using the model phases, was found at the site of the coenzyme position. The *R*-factor before refinement, including all solvent molecules, was 21.4%.

The quinonoid intermediate was modeled into the positive density in the difference electron density map. In order to exclude any bias by a model structure, the ideal stereochemistry, particularly the planarity of the resonance system, was partially suspended to achieve the best possible fit to the observed difference density. Three groups, the quinonoid pyridine ring system including the C4−C4′ double bond and the two carboxyl groups of the ligand moiety, were maintained planar by restraining their geometry in the course of the least-squares refinement. Since there was already some evidence for nonplanarity at the α-carbon atom, its planarity was discarded as a restraint for the refinement. After a few cycles of local refinement (PROLSQ), it became obvious that the model structure had to adopt a tetrahedral configuration around Cα. Positive electron density indicated a fourth bond to the α-carbon atom. Considering the results of the spectrophotometric experiments, only the carbinolamine intermediate has the adequate stereochemistry to fit into the observed electron density; the ketimine structure can be excluded because of its double bond between Cα and the substrate nitrogen. This surprising result was assumed as a working model for the further refinement procedure.

An ideal model for the carbinolamine intermediate was constructed using the program INSIGHT and, again disregarding stereochemical constraints, was optimally modeled into the electron density. The same was done for the side chain of Lys 258.

Coordinates of 358 atoms within a sphere of 9 Å around C4′ were refined using the program PROLSQ; 15 cycles of refinement improved the *R*-factor from 21.40% to 20.92%. An $F_{obs} - F_{calc}$ difference electron density map was examined

Table 2: Parameters of the Final Protein Structural Model[a]

	Sigma (Å)	rms (Å)	number	no. of deviations
bond length (1−2) neighbor	0.02	0.024	3257	554 of all 8818 distances deviate by more than 3σ
angle-related distance (1−3) neighbor	0.04	0.073	4440	
planar (1−4) distance	0.05	0.078	1121	
planar group	0.02	0.016		6 planes deviate by more than 2σ
nonbonded contacts: single torsion contact	0.3	0.216	1150	4 contacts deviate by more than 2σ
multiple-torsion contact	0.3	0.275	1602	43 contacts deviate by more then 2σ

[a] The input standard deviations are given (Sigma) as well as the rms deviations after the refinement and the number of occurrences of each type of atomic coupling and interatomic contacts.

for negative electron density at the position of the Cα-hydroxyl group after cycle 12. None exceeding the background level was found, again corroborating the existence of the Cα-hydroxyl group. The coordinates after cycle 15 served as the starting model for the refinement of the whole molecule. After 10 cycles of refinement of the whole molecule, the *R*-factor dropped from $R = 20.92\%$ to $R = 15.05\%$. Subsequent cyclic refinement of isotropic temperature factors as well as coordinates of all non-hydrogen atoms was performed (10 cycles). An average isotropic *B*-factor of $B = 26.05$ Å^2 was obtained. At $R = 14.3\%$, the *R*-factor did not decrease further without increasing the weighting factor of the crystallographic term and neglecting stereochemical constraints. At this stage (35 cycles of refinement) it seemed reasonable to avoid further deterioration of the geometry. Giving a weighting factor (w) of 0.4 ($w = 1.0$ corresponds to consideration of only the crystallographic term), the model was refined to convergence after a few cycles and the *R*-factor increased to $R = 14.65\%$; 357 water molecules (oxygen atoms) were found. A final difference electron density map proved to be essentially featureless.

Most of the amino acids lie within the allowed areas for L-alanine residues. Ser 107 and Ser 296* were refined to conformations outside the sterically allowed areas as was reported earlier (McPhalen et al., 1992). The γ-OH group of Ser 107 is involved in a hydrogen bond to one of the phosphate oxygens. Ser 296* is known to form a hydrogen bond to a side chain nitrogen of Arg 292*. Both are part of highly irregular loop structures. A list with the relevant parameters of the final protein structural model is given in Table 2.

Carbinolamine Structure. As mentioned before, two experimental observations, namely, evidence for a tetrahedral geometry around Cα in the initial map as well as after refinement and no negative electron density for the hydroxyl group in a difference map, suggested that the crystal was predominantly occupied by the carbinolamine intermediate. A reasonable temperature factor for the hydroxyl group at Cα ($B = 28.9$ Å^2) after cycle 41 provides further evidence. This is a reasonable value in comparison to the isotropic, atomic *B*-factors of the other ligand atoms, varying from 25 to 28 Å^2.

Finally, another approach ruled out the possibility that the density for the critical hydroxyl group had to be attributed to model bias. The whole enzyme structure was refined *de novo*, starting with the initial model, but the ligand atoms, including the coenzyme 4′-carbon, Tyr 70*, and Lys 258, were omitted. So it was avoided that any model bias is introduced at the beginning of the refinement that is "memorized" later on, even if the ligand is set "dummy". The refinement was stopped when the *R*-factor reached a value of $R = 15.27\%$. The difference electron density map

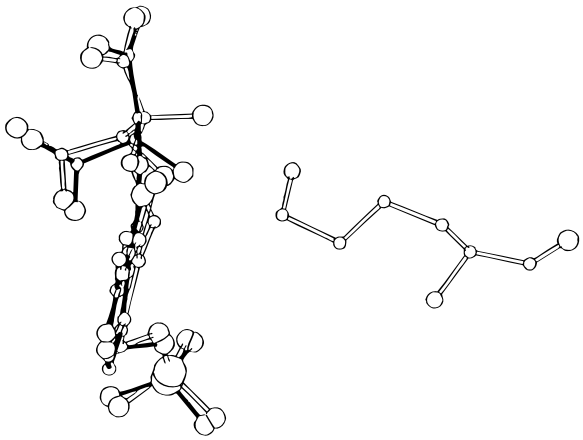

FIGURE 4: Superposition of the quinonoid structure (black bonds) and the carbinolamine structure (open bonds). A slight reorientation of the phosphate group occurs. It occupies a similar position as in the external aldimine. The conformation of Lys 258 is omitted.

($F_{obs} - F_{calc}$) provided unambiguous evidence for the existence of the Cα-hydroxyl group at a contour level of 3σ.

Determination of the Occupancies with TNT. The refinement program package TNT was employed for the simultaneous determination of occupancies of the carbinolamine and the quinonoid. Initially, the occupancy of the carbinolamine structure was tentatively assigned to 80% in accordance with the spectrophotometric results. The quinonoid structure was arbitrarily modeled into the difference between the observed and calculated (80% occupancy of the carbinolamine intermediate) electron density. The quinonoid intermediate is distinguished by its planar geometry due to its conjugated double-bond system. The ligand Cα and Cβ atoms lie within the same plane as the pyridine ring system. The resonating π-bond system is supposed to extend to the α-carboxylate group. On the other hand, in the carbinolamine derivative the cofactor pyridine ring has an aromatic character, but no further double bonds exist. The 4′-carbon, the linking nitrogen, and the α-carbon atom have tetrahedral geometry (sp^3). The α-carbon atom is characterized by an additional hydroxyl group. Coordinates as well as *B*-factors (initially set to $B = 20$ Å^2) of the atoms of the quinonoid structure were refined. It should be emphasized that the *R*-factor had to be dismissed from its function to highlight the progress of refinement; small changes of these parameters did not affect the *R*-factor ($R = 14.7\%$). The result of the simultaneous refinement of the quinonoid form and the carbinolamine form is shown in Figure 4.

Evidently, the quinonoid and the carbinolamine intermediate are distinguished by the hydroxyl group at Cα. It became apparent in the course of refinement cycles, starting with

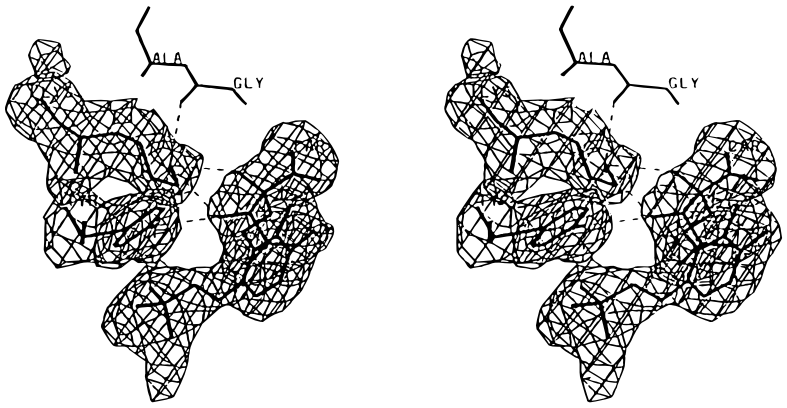

FIGURE 5: Omit map ($F_{obs} - F_{calc}$). The cofactor and the covalently bound substrate as well as Lys 258 and Tyr 70* were omitted for its calculation. The β-oxygen atom and the γ-oxygen atom of the carbinolamine intermediate fit into the electron density. Hydrogen bonds are indicated by dashed lines. While the hydrogen bonds between the ζ-nitrogen atom of Lys 258 and the main chain oxygen of Gly 38, Oη of Tyr 70*, and Oβ of the carbinolamine seem to be likely, the hydrogen bond between Nζ and Oγ is questionable. The hydrogen bond between Oγ and Tyr 70* Oη is shown.

different initial occupancy ratios, that the value of the aforementioned oxygen was always determined to be around 80%. Another calculation corroborated this result, when the initial occupancies of the quinonoid and the carbinolamine form were alternatively set to 100% and only the occupancy of the oxygen was allowed to be refined. Again the refinement of the occupancy of the β-oxygen atom converged to values of approximately 80%. These refinements justify the conclusion that the crystal is occupied for 80% by the carbinolamine intermediate and for 20% by the quinonoid intermediate.

Active Site. The mutual interactions of Gly 38, Lys 258, Tyr 70*, and the carbinolamine complex are especially interesting with regard to the attempt to interpret the inhibition mechanism of *erythro*-β-hydroxyaspartate. Figure 5 shows an omit map ($F_{obs} - F_{calc}$, σ_a-weighted, contour level 3σ). All four aforementioned moieties were omitted from the structure factor calculation for this difference electron density map. The dihedral angle χ4 around Cδ−Cϵ of Lys 258 (defined by Cγ, Cδ, Cϵ, and Nζ) is 31°, and the dihedral angle χ3 around Cγ−Cδ is 172°. Two strong lines of evidence support the correctness of this conformation. First, a well-defined electron density for Nζ can be recognized (Figure 5) as opposed to previous studies with other inhibitors (J. Jaeger, personal communication). Second, alternative model building for the side chain of Lys 258 failed; it was not possible to model another conformation for the side chain of Lys 258 (rotation around its C−C bonds) significantly different from that in Figure 5 without ignoring too short VdW contacts. The low-temperature factor ($B = 18$ Å^2) in comparison to an average *B*-factor of 26 Å^2 of the whole molecule also supports a unique position of the ζ-nitrogen atom. This conformation can be explained by the extensive hydrogen bond network in this region. The hydroxyl group at Cα is hydrogen bonded to the lysine nitrogen. A continuous electron density between these two atoms in the above-cited map (contour level: 1.2σ) corroborates this assumption. The distance between them is 2.8 Å. In fact, no electron density for a water molecule—carrying out a nucleophilic attack on Cα—between Lys 258, Cα, and Tyr 70* was found, as was signaled for the quinonoid intermediate and the ketimine intermediate (Kirsch et al., 1984). This observation is in accordance with the catalytic mechanism. Considering only distance criteria, three further hydrogen bonds are feasible for the ϵ-NH_2 group: (i) to the main chain oxygen of Gly 38 (acceptor, $d = 2.8$ Å), (ii) to the hydroxyl group of Tyr 70* ($d = 2.9$ Å), and (iii) to the substrate *erythro*-β-hydroxyl group ($d = 3.2$ Å). Hydrogen bonds to Gly 38, the carbinolamine Oβ, and hydroxyl group of Tyr 70* can simultaneously be formed without violation of stereochemistry; the tetrahedral geometry around Nζ of Lys 258 can be maintained. Misalignments of energetically ideal hydrogen bonds are within the range of normal deviations in protein structures (Moews & Kretsinger, 1975; Baker & Hubbard, 1984). The possibility to form a hydrogen bond to the substrate γ-oxygen atom should be kept in mind, although geometrical constraints seem to preclude this putative interaction. Finally, the involvement of the side chain of Tyr 70* in two other hydrogen bonds should be noted: to a phosphate oxygen (see above, $d = 2.7$ Å) and to the *erythro*-β-hydroxyl group ($d = 2.6$ Å).

The lysine ϵ-NH_2 group is most probably charged at the stage found in the present crystal structure. Metzler (1979) proposed a stepwise procedure: Lys 258 takes over a water proton. Subsequently, the nucleophilic hydroxyl ion attacks the α-carbon atom which results in the formation of the carbinolamine. Lys 258 functions again as a proton shuttle, protonating the carbinolamine nitrogen and acquiring a proton from the Cα-hydroxyl group (Jansonius & Vincent, 1987).

The tilt angle of the cofactor pyridine ring is similar to that of the external aldimine. The torsion angles around C5−C5′ and C5′−OP1 as well as OP1−P (defined by OP2, P, OP1, and C5′) are 45°, 157°, and 26°, respectively, compared to those of the external aldimine (43°, 161°, and 27°, respectively; Vincent et al., unpublished results).

DISCUSSION

There are two main points of interest in this study. First, *erythro*-β-hydroxyaspartate is known to be a poor substrate that reacts in solution approximately 200-fold slower than the natural substrate (Hammes & Haslam, 1969), but its diastereoisomer, *threo*-β-hydroxyaspartate, was found to be a normal substrate; a structural explanation is sought. Second, the 330/340 nm absorption band of orthorhombic crystals of AAT in the presence of *erythro*-β-hydroxyaspartate can, in principle, arise from three different compounds.

Table 3: Equilibrium Constants, Relative Proportions, and Rate Constants of Intermediate Analogues as Calculated by Hammes and Haslam (1969) for the Reaction of cAAT with *erythro*-β-Hydroxyaspartate[a]

components	K_i (M^{-1})	X_i (%)	k_i (s^{-1})	k_{-1} (s^{-1})
1	284	9.2	3.1×10^6	1.1×10^4
2	0.725	6.6	1.6×10^3	2.2×10^3
3	1.35	9.0	2.1×10^3	1.6×10^3
4	2.17	19.4	1.3×10^3	6×10^2
5	0.304	5.9	1.9×10^2	6.3×10^2
6	5.23	30.9	10.36	1.98
7	0.613	19.0	1.9×10^2	3.1×10^2

[a] They performed rapid reaction kinetics using cytosolic aspartate aminotransferase from pig heart. Component 4 was assigned to the quinonoid structure, and component 5 was assigned to the ketimine structure, whereas further assignments were avoided by the authors. The 30.9% fraction in fact probably represents the carbinolamine form on the basis of the present study.

It was expected that crystallography could help to determine the composition qualitatively and quantitatively. In fact, the latter problem was solved in this work for the mitochondrial isoenzyme. The portion of the 330 nm absorbing component(s) was calculated to be approximately 80%, as independently determined by both UV/vis spectroscopy and X-ray crystallography. The composition of the intermediates absorbing at 330 nm is dominated by the carbinolamine, although minor amounts of ketimine cannot be excluded. At this point, one has to realize the limitations of crystallography. Very low occupancies of closely related structures—as in the case of ketimine in the presence of the carbinolamine—cannot be resolved. No crystallographic indications were found for the existence of the pyridoxamine (PMP) form.

Hammes and Haslam (1969) calculated the equilibrium populations of cytosolic AAT intermediates with *erythro*-β-hydroxyaspartate in solution (Table 3). Assuming that the equilibrium concentrations for the same reaction with mAAT are essentially the same in solution, the orthorhombic crystal exhibits a striking, contrasting accumulation of the carbinolamine structure. It was first considered that the accumulation of the carbinolamine form might somehow be explained by crystal lattice forces modifying the equilibrium concentrations of the intermediates. Thus, the predominant occupancy of the carbinolamine would rather be a general feature of orthorhombic mAAT crystals soaked in substrate solutions than a consequence of the special properties of *erythro*-β-hydroxyaspartate. Picot (1987) soaked orthorhombic crystals of mAAT complexed with maleate in a solution of L-aspartate (100 mM) and found a constant spectrum with a 330 nm absorption band. In the light of this result, crystals of mAAT binding the natural substrate L-aspartate were crystallographically examined. Malashkevich et al. (1993) identified the component absorbing at 330 nm as the ketimine intermediate. Therefore, the carbinolamine is thermodynamically more stable than the ketimine in crystals soaked in solutions of *erythro*-β-hydroxyaspartate and *vice versa* in crystals soaked in solutions of L-aspartate.

The involvement of the hydroxyl group at the Cβ atom in hydrogen bonding offers an explanation for the accumulation of the carbinolamine. A thorough analysis of the network of hydrogen bonds within the active site revealed two possible hydrogen bonds that are potentially relevant to the accumulation of the carbinolamine: one from Oγ of the ligand to the hydroxyl group of Tyr 70* and the other from the same atom to the ϵ-NH_2 group of Lys 258 ($d = 3.2$ Å). The latter is stabilized by hydrogen bonds to the Gly 38 oxygen, to the hydroxyl group of Tyr 70*, and to the α-hydroxyl group of the accumulated carbinolamine. It is tempting to postulate a second hydrogen bond pattern for Lys 258 that could alternatively include the *erythro*-β-hydroxyl group. Omit maps for the active site did not reveal any continuous electron density between Lys 258 and the β-hydroxyl group at a low contour level as in the case of the other hydrogen bonds that had been identified by the program CONTACT (CCP4 program suite) and by the author's examination. Nevertheless, hydrogen bonding of the ϵ-NH_2 group of Lys 258 to the α-hydroxyl group and the *erythro*-β-hydroxyl group would provide a simple explanation for the thermodynamic stability of the carbinolamine.

Another hydrogen bond for the *erythro*-β-hydroxyl group to the hydroxyl group of Tyr 70* at a distance of 2.6 Å was identified in the refined carbinolamine structure. In fact, this strong hydrogen bond might supply another explanation for the accumulation of the carbinolamine, if the bond is absent in the ketimine. The $\Delta\Delta G$ shifting the equilibrium from an occupancy of 80% for the carbinolamine (and, arbitrarily, of 2% for the ketimine) to an occupancy of 80% for the ketimine (and, arbitrarily, of 2% for the carbinolamine) is of the order of magnitude of a strong hydrogen bond (10−15 kJ/mol). Other hydrogen bonds for the β-hyrdoxyl group can be excluded; the nearest phosphate oxygen is at a distance of 3.97 Å.

An unambiguous answer for the cause of the slow transamination of *erythro*-β-hydroxyaspartate cannot be given. Only hypothetic proposals on the kinetic mechanism can be made based on the knowledge of the carbinolamine structure. Hammes and Haslam (1969) used temperature-jump, stopped-flow, and spectrophotometric techniques to study the kinetics of the interaction of aspartate aminotransferase with *erythro*-β-hydroxyaspartate (pig heart cytosolic AAT). Eleven relaxation processes were observed, and eight of them seem to be directly related to the enzymatic reaction. The rate-determining step was tentatively assigned to the hydrolysis or a conformational change of the ketimine. That would mean that the additional *erythro*-β-hydroxyl group causes a change of the rate-determining step in comparison to natural substrates. Kinetic experiments with natural enzyme:substrate intermediates seem to support the proposal that proton abstractions in the tautomerization are the rate-limiting steps (Fang et al., 1970; Julin et al., 1989). It is reasonable that the formation of an additional hydrogen bond to the *erythro*-β-hydroxyl group must be the *ultima ratio* of the altered mechanism. Since the *threo*-β-hydroxyl group exhibits the properties of a kinetically normal substrate, Lys 258 and Tyr 70* are for sterical reasons the candidates for hydrogen donor or hydrogen acceptor functions. Two hypothetical mechanisms of inhibition can be proposed (but others are conceivable). The energy necessary for the breakage of a hydrogen bond could explain a rate constant that is approximately 200 times lower for *erythro*-β-hydroxyaspartate than for aspartate itself. The water molecule attacking the ketimine double bond might form a hydrogen bond to the *erythro*-β-hydroxyl group, slowing down this reaction step. On the other hand, the low reactivity of *erythro*-β-hydroxyaspartate in comparison to aspartate may be due to a hydrogen bond between the *erythro*-β-hydroxyl

group and the ϵ-NH_2 group of Lys 258 at this stage of catalysis preventing its activity as a proton shuttle.

ACKNOWLEDGMENT

The author feels very much obliged to Dr. J. N. Jansonius, Biocentre-Basel University, and Dr. M. Toney for their helpful advice.

REFERENCES

Arnone, A., Rogers, P. H., Hyde, C. C., Briley, R. D., Metzler, G. M., & Metzler, D. E. (1985) *Transaminases*, pp 138−155, J. Wiley & Sons Inc., New York.
Baker, E. N., & Hubbard, R. E. (1984) *Prog. Biophys. Mol. Biol. 44*, 97−179.
Braunstein, A. E. (1973) *The Enzymes*, 3rd ed., Vol. 9, pp 379−481, Academic Press, New York.
Christen, P., & Metzler, D. E. (1985) *Transaminases*, John Wiley & Sons Inc., New York.
Cleland, W. W. (1963) *Biochim. Biophys. Acta 67*, 104−137.
Craig, D. P., & Walmsley, S. H. (1968) *Excitons in Molecular Crystals*, chapter 1, pp 1−22, W. A. Benjamin, Inc., New York.
Eichele, G. (1980) Ph.D. Thesis, Universität Basel.
Eichele, G., Karabelnik, D., Halonbrenner, R., Jansonius, J. N., & Christen, P. (1978) *J. Biol. Chem. 253*, 5239−5242.
Eichele, G., Ford, G. C., Glor, M., Jansonius, J. N., Mavrides, C., & Christen, P. (1979) *J. Mol. Biol. 133*, 161−180.
Fang, S.-M., Rhodes, H. J., & Blake, M. (1970) *Biochim. Biophys. Acta 212*, 281−287.
Fasella, P., & Hammes, G. G. (1967) *Biochemistry 6*, 1798.
Ford, G. C., Eichele, G., & Jansonius, J. N. *(1980) Proc. Natl. Acad. Sci. U.S.A. 77*, 32−51.
Gehring, H. (1986) *Eur. J. Biochem. 159*, 291−296.
Gehring, H., Christen, P., Eichele, G., Glor, M., Reimer, A.-S., Smit, J. D. G., Thaller, C. (1977) *J. Mol. Biol. 115*, 97−101.
Hammes, G. G., & Haslam, J. L. (1969) *Biochemistry 8*, 1591−1598.
Hartshorne, N. H., & Stuart, A. *Practical Optical Crystallography*, chapter 2, pp 47−108, E. Arnold, Ltd., London.
Haruff, R., & Jenkins, T. W. (1978) *Arch. Biochim. Biophys. 188*, 37−46.
Harutyunyan, E. G., Malashkevich, V. I., Kochkina, V. M., & Torchinsky, Y. M. (1985) *Transaminase*, pp 164−173, J. Wiley & Sons Inc., New York.
Hendrickson, W. A., & Konnert, J. H. (1980) in *Computing in Crystallography* (Diamond, R., et al., Eds.), Indian Academy of Sciences, International Union of Crystallography, India.
Hughes, R. C., Jenkins, T. W., & Fischer, E. H. (1962) *Proc. Natl. Acad. Sci. U.S.A. 48*, 1615−1618.
Jansonius, J. N., & Vincent, M. G. (1987) *Biol. Macromol. Assem. 3*, 187−285.
Ivanov, V. I., & Karpeisky, M. Y. *(1969) Adv. Enzymol. 32*, 21−53.
Jenkins, W. T. (1961) *J. Biol. Chem. 234*, 1121−1125.
Jenkins, W. T. (1964) *J. Biol. Chem. 239*, 1743−1747.
Jenkins, W. T. (1979) *Anal. Biochem. 93*, 134−138.
Jenkins, W. T., Yphantis, D. A., & Sizer, I. W. (1959) *J. Biol. Chem. 234*, 51−57.
Julin, D. A., & Kirsch, J. F. (1989) *Biochemistry 28*, 3825−3833.
Karpeisky, M. Y., & Ivanov, V. I. (1966) *Nature 210*, 493−496.
Kirsch, J. F., Eichele, G., Ford, G. C., Vincent, M. G., Jansonius, J. N., & Christen, R., Gehring, H. (1984) *J. Mol. Biol. 174*, 497−525.
Konnert, J. H. (1976) *Acta Crystallogr. A 32*, 614−617.
Malashkevich, V. N., & Sinitza, N. I. (1991) *J. Mol. Biol. 221*, 61−63.
Malashkevich, V. N., Toney, M. D., & Jansonius, J. N. (1993) *Biochemistry 32*, 13451−13462.
McPhalen, C., Vincent, M. G., & Jansonius, J. N. (1992) *J. Mol. Biol. 225*, 495−517.
McPherson, A. (1976) *J. Biol. Chem. 251*, 6300−6303.
McPherson, A. (1982) *Preparation and Analysis of Protein Crystals*, p 94, J. Wiley & Sons Inc., New York.
Messerschmidt, A., & Pflugrath, J. W. (1987) *J. Appl. Crystallogr. 20*, 306−315.
Metzler, D. E. (1979) *Adv. Enzymol. 50*, 1−40.
Metzler, C. M., & Metzler, D. E. (1987) *Anal. Biochem. 166*, 313−327.
Metzler, C. M., Mitra, Y., & Metzler, D. E. (1988a) *J. Mol. Biol. 203*, 197−220.
Metzler, C. M., Harris, A. G., & Metzler, D. E. (1988b) *Biochemistry 27*, 4923−4933.
Mitra, R., Metzler, C. M., & Metzler, D. E. (1989) *Arch. Biochem. Biophys. 270*, 526−540.
Moews, P. C., & Kretsinger, R. H. (1975) *J. Mol. Biol. 91*, 201−228.
Picot, D. (1987) Ph.D. Thesis, Universität Basel.
Picot, D., Sandmeier, E., Thaller, C., Vincent, M. G., Christen, P., & Jansonius, J. N. (1991) *Eur. J. Biochem. 196*, 329−241.
Schirch, L. V., & Slotter, R. A. (1966) *Biochemistry 5*, 3175−3181.
Snell, E. E. (1962) *Brookhaven Symp. Biol.* 15.
Taylor, J. E., Metzler, D. E., & Arnone, A. (1990) *Vitamin B_6*, p 585, Annals of the New York Academy of Science, New York.
Ten Eyck, L. F. (1977) *Acta Crystallogr.* 486−492.
Thomas, D., van der Putten, N., & Kiers, C. (1986) *Manual of FAST diffractometer*, ENRAF NONIUS, Delft, The Netherlands.
Toney, M. D., & Kirsch, J. F. (1989) *Science 243*, 1485−1488.
Ulevitch, R. J., & Kallen, R. G. (1977) *Biochemistry 16*, 4351−4354.

BI960994Z